Rotationally invariant double pulsed field gradient diffusion imaging

Sune Nørhøj Jespersen[1,2], Henrik Lundell[3], Casper Kaae Sønderby[3], and Tim B. Dyrby[3]
[1]*CFIN/MINDLab, Aarhus University, Aarhus, Denmark,* [2]*Department of Physics, Aarhus University, Aarhus, Denmark,* [3]*Danish Research Centre for Magnetic Resonance, Copenhagen University Hospital Hvidovre, Hvidovre, Denmark*

Introduction: Pulsed field gradient diffusion sequences (PFG) with two diffusion encoding blocks separated by a variable delay (mixing time) have been shown to have the ability to detect nonspherical pore shapes ("pore shape anisotropy" or "microscopic anisotropy") in macroscopically isotropic samples[1-5]. One such approach is *angular* double PFG (d-PFG), where pore shape anisotropy manifests itself in a signal modulation as the angle θ between the two diffusion encoding directions is varied. However, current approaches to quantifying compartment shape anisotropy using angular d-PFG are not rotationally invariant and are affected by pore orientation anisotropy when applied to macroscopically anisotropic systems[5-7]. Here we propose a new and rotationally invariant sampling scheme of d-PFG, allowing estimation of orientation distribution independent quantities. The sampling scheme is evaluated with numerical simulations and ex vivo experiments on a vervet monkey brain.

Theory In angular d-PFG, the diffusion wave vector magnitude q of the 2 diffusion encoding blocks is kept equal, while their relative angle θ is varied. When the sample is isotropic and the mixing time sufficiently long, the modulation of the d-PFG signal $S^{\text{iso}}(q,\theta)$ with θ is known to reflect microscopic anisotropy. In fact, the amplitude ε of the modulation is a measure of pore shape anisotropy, and it can be determined by forming the difference between the log signals of two diffusion measurements, one with parallel and one with perpendicular diffusion wave vectors: $\varepsilon q^4 = \log S^{\text{iso}}(q,0) - \log S^{\text{iso}}(q,\pi/2)$. However, in anisotropic ensembles, this difference depends not only on pore shape anisotropy, but also on macroscopic anisotropy and absolute wave vector orientations. This dependency can be removed by averaging the signal $S(\mathbf{q}_1,\mathbf{q}_2)$ over all possible orientations. Using the theory of exact quadrature on the rotation group[8], we find that this average (S^{iso}) can be determined exactly up to 6th order in q by sampling the d-PFG using only 60 rotations ($\mathrm{R} \in \chi$) of an arbitrary set $(\hat{e}_1,\hat{e}_2)$ of unit vectors with relative angle θ

$$S^{\text{iso}}(q,\theta) = \frac{1}{60}\sum_{\mathrm{R}_i \in \chi} S(\mathrm{R}_i q\hat{e}_1, \mathrm{R}_i q\hat{e}_2) \quad (1)$$

For the case of perpendicular wave vectors $\theta = \pi/2$, the directions of the first wave vector $\mathbf{q}_1$ correspond to the 12 vertices of the icosahedron (Fig. 1a), while the 2nd wave vector $\mathbf{q}_2$ samples 5 equidistant points on the corresponding great circle (Fig. 1b), resulting in a total of 12 x 5 = 60 directions. The directions of the 2nd wave vector associated with 2 anti-podal directions of the first diffusion wave vector make up 10 uniformly distributed directions on the great circle (Fig. 1b). For the case of parallel wave vectors, the directions are the 12 vertices of the icosahedron. Thus, a quantitative and rotationally invariant measure of pore shape anisotropy ε can be estimated from 72 pairs of directions by

$$\varepsilon q^4 = \log(1/12\sum_{\mathrm{R}_i \in \chi} S(\mathrm{R}_i q\hat{e}_x, \mathrm{R}_i q\hat{e}_x)) - \log(1/60\sum_{\mathrm{R}_i \in \chi} S(\mathrm{R}_i q\hat{e}_x, \mathrm{R}_i q\hat{e}_y)) + O(q^6) \quad (2)$$

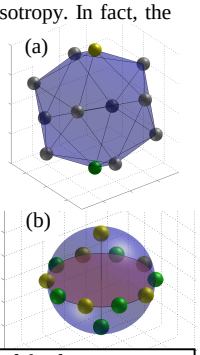

Fig. 1 Directions of the first wave vector (a), and associated orthogonal wave vectors (b), matched to the first (North and South pole) according to color.

Methods: Monte Carlo simulations of diffusion in spheroids were implemented in Matlab using 50,000 particles, D = 2 µm²/ms, and time step 1 µs. The spheroids had long semi-axes of 2, 4 or 8 µm and short semi-axis 1 µm. The orientations of the long axes of the cylinders were sampled from a Watson distribution, with concentration parameters κ ranging from 0 to 20 (uniform to highly concentrated distributions). Diffusion times ranged from 0 to 400 ms, mixing times was set to the maximum diffusion time in each case, and diffusion wave vector q from 0 to 5 µm^{-1}. We compare ε to an analogous index of microscopic anisotropy, IMA, of pore shape anisotropy introduced in [5]. A spin echo double PFG sequence was implemented on a Varian 4.7 T scanner, and images of a perfusion fixed vervet monkey brain prepared as in[9] were acquired using Δ/δ = 11/3 ms, mixing time 15 ms, resolution 0.6 mm isotropic, and diffusion gradient G = 0.49T/m. Number of averages was 2 and total acquisition time was 46 hours. Two additional acquisitions were collected, one in which the set of diffusion directions were rotated in order to assess rotational invariance, and one with a lower diffusion gradient G = 0.346 T/m to address robustness.

Results: Simulations from different Watson distributions demonstrated ε to be independent of macroscopic anisotropy, and to be relatively robust against variations in diffusion time (Fig. 2). In terms of the diffusion wave vector, there was a larger window of accuracy for ε than for IMA. In Fig. 3, a coronal slice of ε is shown – note that it is predominantly positive as it should be, and that it is generally larger in white matter. Finally, in Fig. 4 we show average ROI values for 6 distinct anatomical regions, corpus callosum (CC), corticospinal tract (CST), motor cortex (M1), somatosensory cortex (SOMAT), putamen (PUT) and caudate nucleus (CD). Note that ε is relatively robust against rotations, but change somewhat when lowering the diffusion weighting G. This latter effect is familiar from other microstructural diffusion indices[10]. Nevertheless, both rotations and variations in G preserve the relationships among the ROI averages. Figure 4 further demonstrates that microscopic anisotropy is larger in white matter than in gray matter [11, 12]. Furthermore, it is larger in corpus callosum than in the corticospinal tract, and among the gray matter regions, motor cortex shows the highest microscopic anisotropy, and deep gray matter the lowest [13].

Conclusions: We presented and evaluated a simple experimental procedure to obtain a precise and rotationally invariant determination of pore shape anisotropy in the presence of macroscopic anisotropy. The procedure involves the acquisitions of a set of only 72 pairs of diffusion directions. We obtained images of pore shape anisotropy in a fixed vervet brain, and values in different anatomical ROIs.

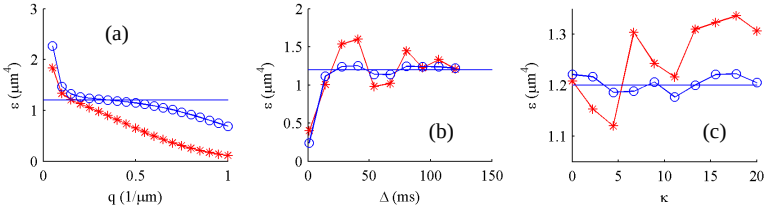

Fig. 2 Microscopic anisotropy ε (blue circles) for spheroids with long semi-axes of 4 µm: IMA (red asterisk), and theoretical value (blue line). In (a), Δ = 120 ms and κ = 0; in (b), q = 0.3 µm^{-1} and κ = 0; (c) Δ = 120 ms and q = 0.3 µm^{-1}.

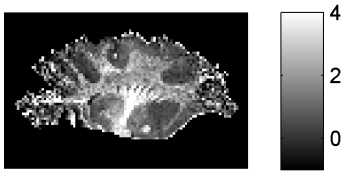

Fig. 3 Parametric map of ε.

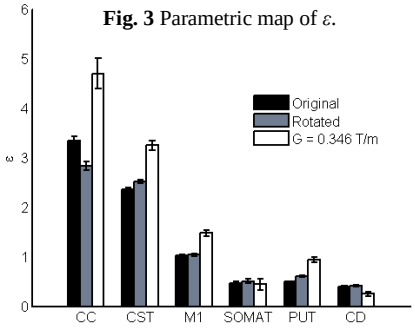

Fig. 4 ROI averages.

References
1. Cheng, Y. and D.G. Cory, J. Am. Chem. Soc., (1999). **121**;2. Mitra, P.P., Phys. Rev. B, (1995). **51**;3. Shemesh, N., et al., NMR Biomed, (2011). **25**;4. Özarslan, E., J. Magn. Reson., (2009). **199**;5. Lawrenz, M., et al., J. Magn. Reson., (2010). **202**; 6. Jespersen, S.N., NMR Biomed, (2012). **25**;7. Jespersen, S.N. and N. Buhl, J. Magn. Reson., (2011). **208**;8. Graf, M. and D. Potts, Numer Func Anal Opt, (2009). **30**;9. Dyrby, T.B., et al., Hum Brain Mapp, (2011). **32**;10. Dyrby, T.B., et al. Magn. Reson. Med., (2012);11. Komlosh, M.E., et al., J. Magn. Reson., (2007). **189**;12. Lawrenz, M. and J. Finsterbusch, Magn Reson Med, (2011). **66**; 13. Shemesh, N., et al., Magn Reson Med, (2012). **68**;